Adsorption and reaction of CH_3COOH and CD_3COOD on the MgO(100) surface: A Fourier transform infrared and temperature programmed desorption study

Cite as: J. Chem. Phys. **102**, 8158 (1995); https://doi.org/10.1063/1.469227
Submitted: 15 August 1994 . Accepted: 27 January 1995 . Published Online: 04 June 1998

Chen Xu, and Bruce E. Koel

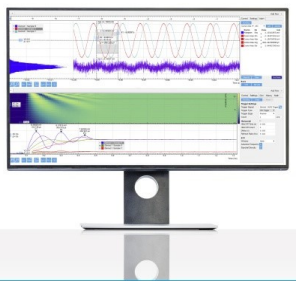

Adsorption and reaction of CH_3COOH and CD_3COOD on the MgO(100) surface: A Fourier transform infrared and temperature programmed desorption study

Chen Xu and Bruce E. Koel
Department of Chemistry, University of Southern California, Los Angeles, California 90089

(Received 15 August 1994; accepted 27 January 1995)

The adsorption of acetic acid (CH_3COOH and CD_3COOD) on the (100) surface of a MgO single crystal has been studied using primarily Fourier transform infrared transmission absorption spectroscopy and temperature programmed desorption (TPD). Acetic acid dissociates upon adsorption on this surface, even at 120 K, forming an adsorbed acetate (CH_3COO) species. Upon heating in TPD, some of the acetate recombines with surface hydrogen and desorbs as acetic acid but most undergoes a disproportionation reaction to form acetic acid and ketene (CH_2CO) products which desorb. The IR intensities of the vibrational modes of chemisorbed acetate over the temperature range of 425–720 K show a strong polarization dependence on the incident IR light indicating an oriented, monodentate adsorbed species. Consideration of the vibrational frequencies of this species reveals new insight concerning the structure and bonding of the acetate radical on the MgO(100) surface and supports our proposal of a novel bimolecular surface reaction between two adsorbed acetate radicals to form ketene and water. © *1995 American Institute of Physics.*

I. INTRODUCTION

The surface chemistry of metal oxides has always attracted a lot of attention because of their wide use in catalysis either as supports or active components.[1–4] Due to the intrinsic complexity of oxide surfaces and experimental difficulty of using electron and ion spectroscopy for analysis of insulating materials, studies using a surface science approach are limited, although they are essential for an understanding of the catalysis on oxide surfaces at the molecular level.[1–4]

To circumvent problems associated with samples of an insulating material, two approaches have been used in the past. The first, which has been recently exploited extensively, is growth of a well-ordered thin oxide film on a metal substrate.[3,5–20] The thin oxide film has, on the one hand, sufficient electrical and thermal conductivity to perform electron spectroscopy and other surface science experiments and on the other hand represents the structure of bulk oxide samples. The second method utilizes an electron gun producing a low current of electrons with a high energy to stabilize charging of the sample during electron spectroscopy.[21–23] In identifying adsorbed species and determining adsorption geometry, high resolution electron energy loss spectroscopy (HREELS) as a vibrational spectroscopy has been particular useful and extensively used on metal surfaces. However, the presence of the so-called Fuchs–Kliewer phonons (surface optical phonons) make applications of HREELS on oxide surfaces very difficult. Wu *et al.*[14] utilized high energy electrons (~50 eV) experimentally to suppress the intensity of the optical phonons in favor of adsorbate-induced losses, while Cox *et al.*[24] and Petrie and Vohs[25,26] used Fourier spectral deconvolution to remove phonon peaks from the measured spectra. Both methods have been successfully applied on a number of oxide surfaces.[14–17,25,26]

Another possibility for studying adsorbates on insulating materials is to utilize optically based methods that involve no charged particles. For instance, infrared (IR) spectroscopy has been extensively used on oxide surfaces.[3,27] Recently, the adsorption of small molecules such as CO, CO_2, and H_2O on single crystal ionic insulators has been studied by a number of groups using IR spectroscopy.[3] In this paper, we combine Fourier transform IR (FTIR) absorption spectroscopy in a transmission mode (ITAS) and temperature programmed desorption (TPD) mass spectrometry to study the adsorption of acetic acid on an ''in-air cleaved,'' bulk, single crystal of MgO. We demonstrate easy access to adsorbate vibrations between 1000 and 3000 cm^{-1} with IR and the ability to obtain detailed information regarding adsorbed species, adsorption geometry, and surface reaction pathways. We also point out that the multiphonon cross section in IR is much lower than in HREELS, and the surface phonon can not even be directly excited by IR.[28]

A wealth of information exists in the literature regarding the interaction of acetic acid on the MgO(100) surface.[15,26,29–33] Parrott *et al.*[29] studied acetic acid adsorption on MgO powders by TPD. Walmsley studied acetic acid adsorption on polycrystalline MgO using inelastic electron tunneling spectroscopy (IETS).[30] More recently, Peng and Barteau investigated the adsorption of acetic acid on MgO(100) using TPD, XPS, and ISS.[31–33] The adsorption of acetic acid on MgO(100) has also been studied by Petrie and Vohs using HREELS.[26] Wu and Goodman studied acetic acid adsorption on epitaxially grown MgO(100) films on a Mo(100) substrate.[15] In all of these studies, which were carried out above 300 K, acetic acid was consistently found to dissociate on the MgO(100) surface upon adsorption, forming acetate and hydroxyl groups. TPD shows a high selectivity for acetic acid dehydration at high temperature on both single crystal and powder MgO surfaces.[29,32] HREELS results for acetic acid adsorbed on MgO(100)/Mo(100) reveal that acetate from acetic acid is stable on the surface up to 600 K.[15] Despite all of this information, no determination exists of the adsorption geometry of adsorbates important in the

 0021-9606/95/102(20)/8158/9/$6.00

acetic acid dehydration mechanism on MgO. This information is crucial to a fuller understanding of the bonding of these species on the surface and the catalytic chemistry of MgO. This paper extends acetic acid adsorption studies to lower temperatures and reports our use of a new FTIR apparatus in our laboratory to elucidate this information.

II. EXPERIMENTAL SECTION

These studies were carried out in a versatile UHV chamber and FTIR apparatus which can carry out IR studies in transmission or reflection modes under UHV conditions or at higher pressures.[34] Briefly, the system is equipped with a Mattson Galaxy 6020 FTIR spectrometer, optics for low energy electron diffraction (LEED), a shielded UTI 100C quadrupole mass spectrometer (QMS) for temperature programmed desorption, and a double-pass cylindrical mirror analyzer (CMA) for Auger electron spectroscopy (AES). The system is pumped by a 240 *l*/s ion pump, a titanium sublimation pump, and a 240 *l*/s turbomolecular pump. The system base pressure was 8×10^{-11} Torr.

TPD measurements were made using the QMS in line-of-sight with the sample surface and using a low, linear heating rate of 2 K/s to insure homogeneous heating of the sample. A screen biased by -55 V was placed between the QMS ionizer and the sample to suppress low energy electrons coming out of the QMS. IR measurements were performed in the transmission mode utilizing both sides of the sample to adsorb molecules. The IR spectra were taken using 8 cm^{-1} resolution and 1000 scans in a 4 min period. In some cases, many experiments under the same conditions were done subsequently and on different days. Signal-averaged spectra comprised of several of these different experiments are shown in this paper.

The MgO(100) crystal (Atomergic, 12 mm$\times$12mm$\times$1.5 mm) was cleaved in air on both sides of the sample. The crystal was mounted tightly via Ta clips in a Ta ''frame'' that was attached to Cu feedthrough rods that were used for resistive heating and were in direct contact with liquid nitrogen. The crystal could be cooled to 110 K or heated to 1000 K. The temperature was measured by a chromel–alumel thermocouple spotwelded on the Ta sample holder. The major contamination on the MgO surface after mounting the crystal in UHV was carbon. The MgO(100) surface was cleaned by annealing the sample at 950 K in 1×10^{-5} Torr O_2. AES was used to check the cleanliness of the surface. Typical AES spectra of the surface before and after oxygen treatment are shown in Fig. 1. A sharp (1$\times$1) LEED pattern was always observed, but there was a relatively high background intensity compared to our experience with metal substrates.

CH_3COOH (Mallinckrodt, 99.9%) and CD_3COOD (Aldrich, 99.5%) were used as received after several freeze-pump-thaw cycles. The purity was checked *in situ* by IR and mass spectroscopy. Acetic acid was exposed on the sample by using a microcapillary array, directed-beam doser in conjunction with a leak valve. The dosing for IR measurements was carried out subsequently on both sides of the sample. To insure similar coverages on both sides (surfaces) of the crystal, in many cases more than one monolayer acetic acid was dosed on both sides and then the surface was annealed to a given temperature for IR measurements. Exposures for TPD studies are given in Langmuirs (1 L$=10^{-6}$ torr sec) without correction for the doser enhancement, ion gauge sensitivity, or other factors. Before gas exposures, the MgO sample was typically flashed to 900–950 K and then cooled down for dosing.

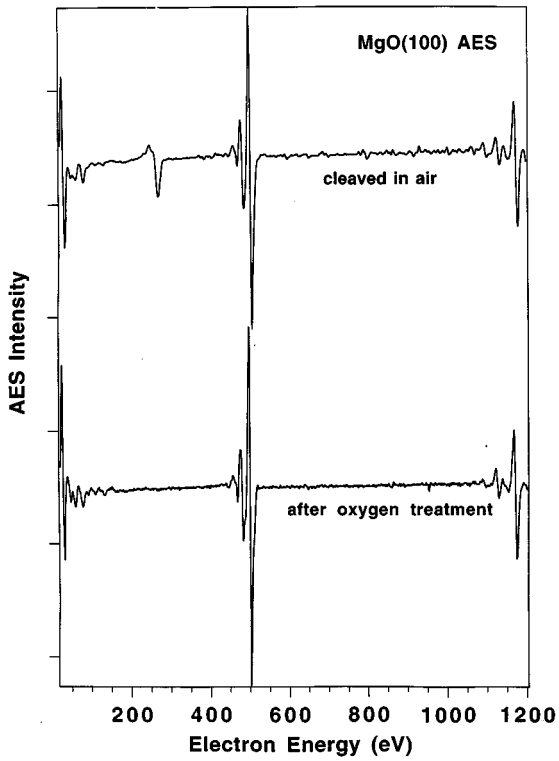

FIG. 1. AES spectra of the MgO(100) sample as initially mounted and after cleaning in UHV using O_2.

III. RESULTS

A. Temperature programmed desorption studies

We utilized the TPD technique to provide essential information on the adsorption, desorption, and reaction of acetic acid on the MgO(100) surface. Prior studies of this system have all been carried out for adsorption temperatures above 300 K. TPD spectra after increasing CH_3COOH exposures on MgO(100) at 120 K are shown in Figs. 2–4. In addition to these curves the mass spectrometer signals at 2, 13, 15, 16, 20, 28, 41, 42, 44 a.m.u. were also monitored but are not shown. From all of these curves, it is evident that three different TPD spectra are present. Signals at 14, 42, and 28 a.m.u. follow the same shape, while 60 and 43 a.m.u. curves show a similar trace. The curve for 18 a.m.u. has very similar peaks to those at 14, 42, and 28 a.m.u. except for an additional peak between 200–300 K. The other curves show little intensity and mostly arise from the cracking patterns of gases monitored by the above-mentioned signals. As examples of these three different traces, we show curves for 60 a.m.u. in Fig. 2, 43 a.m.u. in Fig. 3, and 14 and 18 a.m.u. in Fig. 4. The TPD spectra in Fig. 4 have been corrected for

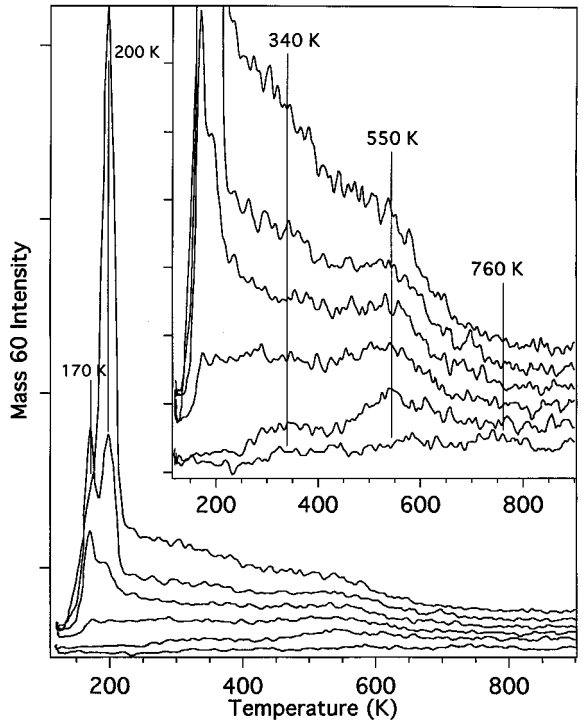

FIG. 2. CH_3COOH TPD curves obtained by monitoring the 60 a.m.u. signal after increasing CH_3COOH exposures.

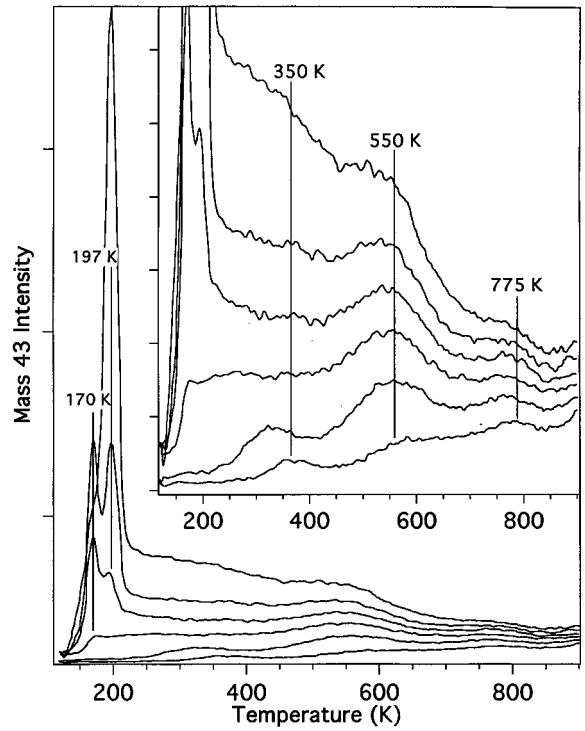

FIG. 3. CH_3COOH TPD curves obtained by monitoring the 43 a.m.u. signal after increasing CH_3COOH exposures.

changes in the baseline. In Figs. 2 and 3, the high temperature features are shown in an expanded view. As one can see, the two major fragmentation products of acetic acid at 60 and 43 a.m.u. follow very similar traces except for the high temperature peak at 775 K which is more prominent for 43 a.m.u. This latter peak is due to a cracking fraction of the product ketene in the QMS (*vida infra*). At small acetic acid exposures, two molecular desorption peaks of acetic acid are observed at 350 and 550 K. Both peaks gain in intensity with increasing acetic acid exposures. In addition, two low temperature peaks appear at 170 and 200 K. The peak at 200 K cannot be saturated with further increased exposures and is attributed to multilayer desorption. It is interesting to note that the peak at 170 K is populated before the desorption state at 200 K, even though it has a lower desorption temperature, and its intensity decreases at higher acetic acid coverages. These two peaks are probably due to different phases of condensed acetic acid, since acetic acid can be present in many chemical states as monomers, cyclic dimers, open chain dimers or in a long chain form, but could also signal differences in the crystallinity of the film. Because of the different hydrogen bonding interactions, small differences in the condensation energy might be present and noticeable as the film thickness increases.

In Fig. 4, TPD spectra monitoring ketene and water formation (desorption) are provided. We assign the signal at 14 a.m.u. to ketene desorption since curves for 14, 28, and 42 a.m.u.—three major cracking products of ketene in the QMS—follow exactly the same traces in TPD. Two ketene desorption peaks at 600 and 775 K were observed at lower acetic acid exposures. At higher acetic acid coverages, we also observed a peak at 400 K. This peak, however, was not saturated even at very high acetic acid exposures. We assign this peak to desorption from the sample holder and not relevant to chemistry on the MgO surface. This assignment is consistent with IR results which do not show large intensity changes around 400 K. Peaks near 200 K are due to cracking products associated with acetic acid desorption.

Water shows very similar TPD curves at temperatures higher than 400 K. However, a peak was also observed at 345 K which gains intensity and shifts to lower desorption temperature with increasing acetic acid exposures. This low

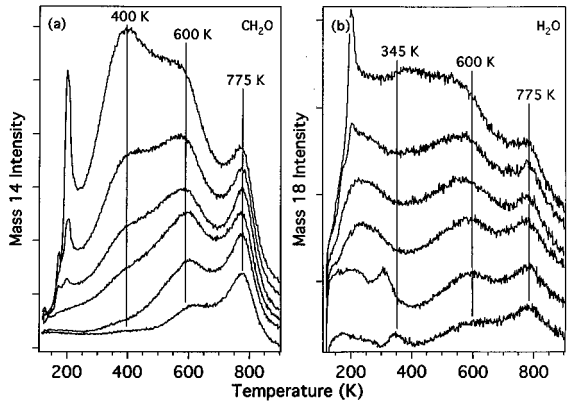

FIG. 4. Ketene (CH_2CO) and water (H_2O) TPD curves after increasing CH_3COOH exposures. Ketene and water are monitored by using signals at 14 and 18 a.m.u., respectively.

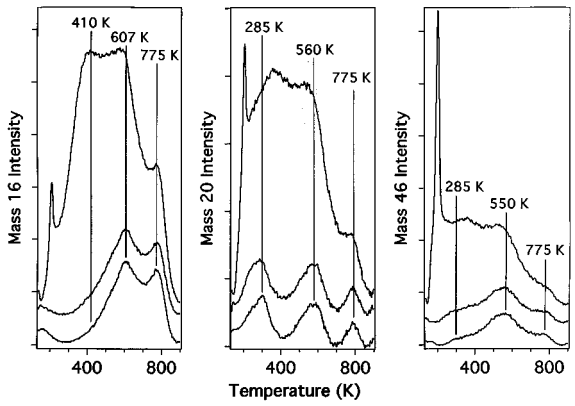

FIG. 5. Ketene (CD_2CO), water (D_2O), and acetic acid (CD_3COOD) TPD curves after increasing CD_3COOD exposures. Ketene, water, and acetic acid are monitored by using signals at 16, 20, and 46 a.m.u., respectively.

temperature peak is very similar to that for TPD of H_2O after H_2O exposures.[15,16]

To verify these results and the assignments made above, TPD spectra after dosing perdeuteroacetic acid (CD_3COOD) were also taken. The results are provided in Fig. 5. Consistent with the above assignments, the signals at 16, 28, and 44 a.m.u. follow the same traces, while those at 46 and 64 a.m.u. show a similar shape. As an example, we only show those curves for 16, 20, and 46 a.m.u. in Fig. 5. One can see that the TPD spectra after perdeutero-acetic acid exposures are the same as those after perhydrido-acetic acid exposures; no significant isotope effect was observed. These results also show that the water desorption peak at 300 K is due to the dissociation of acetic acid on the surface, rather than due to the adsorption of water from the background gas in the chamber.

We directly compare the TPD spectra of water, ketene, and acetic acid after dosing perdeutero-acetic acid onto the surface in Fig. 6. The QMS intensity for characteristic ketene and water cracking products is larger than that for the acetic acid cracking product by a factor of 10. Without correcting

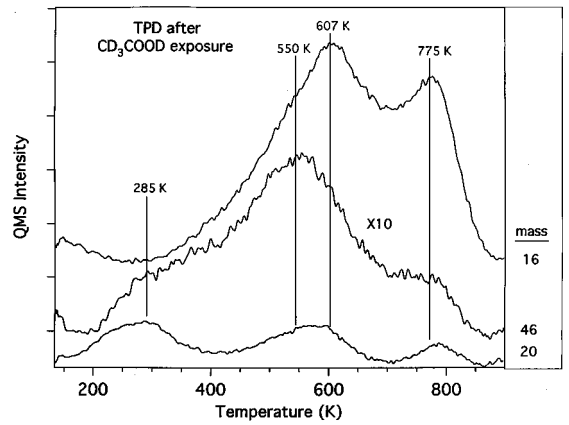

FIG. 6. Comparison of ketene (CD_2CO), water (D_2O), and acetic acid (CD_3COOD) TPD curves after a CD_3COOD exposure that produces a monolayer on the surface. Ketene, water, and acetic acid are monitored by using signals at 16, 20, and 46 a.m.u., respectively.

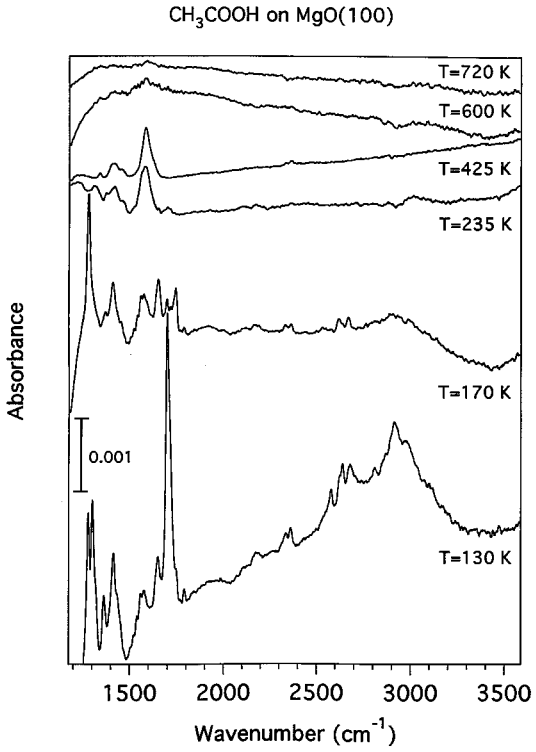

FIG. 7. FT-ITAS spectra of acetic acid on MgO(100) taken after dosing 2.5 layers of CH_3COOH and subsequently annealing to the indicated temperatures.

for the different sensitivities or careful quantification, one can roughly say that ketene and water are the major gas phase products of acetic acid reaction at temperatures higher than 400 K. This is consistent with the previous TPD results of Peng and Barteau[32] who observed a 100% selectivity for acetic acid dehydration on this surface. However, as one can see in Fig. 6, a significant amount of acetic acid also molecularly desorbs from the surface in our experiments. The water desorption peak at 285 K was not observed previously by Peng and Barteau[32] because their TPD experiments were carried out at temperatures above 300 K. Finally, the AES spectra after these TPD experiments showed a clean surface, indicating complete desorption of all adsorbed species resulting from acetic acid adsorption and reaction.

B. Infrared spectroscopy studies

We also studied the adsorption of acetic acid on MgO(100) with FTIR in the transmission-absorption mode in order to elucidate information on the structure and bonding of the adsorbed layer. Figure 7 shows an annealing series of these spectra taken after dosing 2–3 layers of CH_3COOH on each of the two sides of the MgO sample at 130 K and subsequently annealing the sample to the indicated temperature. The spectra were taken with p-polarized light at an incident angle, α, of 0° between the surface normal and the incident IR beam. The multipeak structure above 2500 cm^{-1} is very characteristic of strongly hydrogen-bonded acetic acid.[35,36] In such cases, the O–H stretching frequency decreases from about 3600 cm^{-1} for the "free" O–H group to

TABLE I. Vibrational assignments for molecularly adsorbed CH_3COOH on MgO(100).

Frequency (cm^{-1})	Mode assignment
1279	δ_{O-H} monolayer or second layer
1302	δ_{O-H} multilayer
1364	ν_{C-O}
1416	δ_{CH_3}
1432	δ_{CH_3}
1570	$\nu_{C=O}$ monolayer or second layer
1653	$\nu_{C=O}$ chain form, monolayer, or second layer
1701	$\nu_{C=O}$ dimer in multilayer
1746	$\nu_{C=O}$ monomeric form, monolayer, or second layer

about 3000 cm^{-1} and overlaps the C–H stretch vibrations. The sharp peaks between 2500 and 2800 cm^{-1} have been attributed to combination bands of lower-frequency vibrations involving the COOH group and the intensity is enhanced by a Fermi resonance with the OH fundamental.[37,38]

In the spectrum obtained at 130 K at least seven peaks can be clearly identified between 1100 and 2000 cm^{-1}: 1279, 1302, 1364, 1416, 1570, 1653, and 1701 cm^{-1}. Two shoulders at 1432 and 1746 cm^{-1} can also be observed. These results are also presented in Table I. To facilitate the assignment of the observed peaks, the FTIR spectra of 2–3 layers of acetic acid at 130 K is compared with thicker, multilayer films of CH_3COOH and CD_3COOD in Fig. 8. From this comparison, the peaks at 1279, 1570, and 1746 cm^{-1} can be correlated to the monolayer or second layer, both of which are modified by the surface. Going from acetic acid to perdeutero-acetic acid, peaks at 1279, 1302, 1416, and 1432 cm^{-1} disappear completely indicating that their origins are vibrations with significant amplitude of motion for H atoms. Therefore, the peaks at 1570, 1653, 1701, and 1746 cm^{-1} can be correlated to a C=O vibration of adsorbed acetic acid in different forms. The peaks at 1416 and 1432 cm^{-1} can be assigned to the C–H deformation of the methyl group. These assignments are consistent with previous results for liquid, solid, and adsorbed acetic acid. However, we assign the peak at 1364 cm^{-1} to a C–O vibration and the peaks at 1279 and 1302 cm^{-1} to O–H deformations. These assignments disagree with those given for IR studies of crystalline acetic acid where the peak at 1284 cm^{-1} was assigned to a C–O vibration and the peak at 1418 cm^{-1} to an O–H deformation.[35,36] However, support for our assignment comes from the work of Gao and Hemminger[39] who found a C–O vibration at 1318 cm^{-1} and an O–H deformation at 1176 cm^{-1} for adsorbed acetic acid on Pt(111), and Chen *et al.*[40] who found a C–O vibration at 1350 cm^{-1} and an O–H deformation at 990 cm^{-1} for adsorbed acetic acid on Al(111).

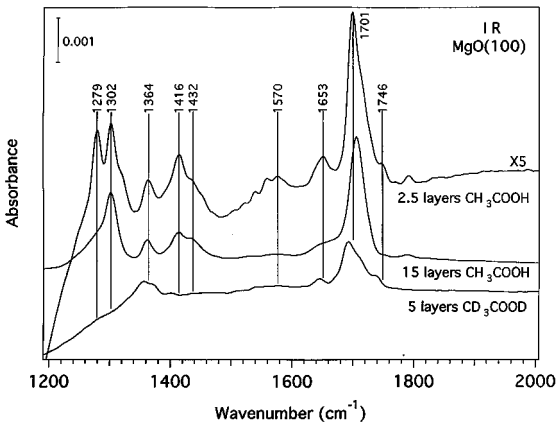

FIG. 8. Comparison of FT-ITAS spectra of CH_3COOH and CD_3COOD multilayers on MgO(100).

As one can see from Fig. 7, the peaks at 1302 and 1701 cm^{-1} disappear almost completely upon annealing to 170 K, while the peaks at 1364, 1416, and 1432 cm^{-1} lose intensity. With further heating to 235 K, the peaks at 1279, 1653, and 1746 cm^{-1} disappear completely and the intensity of the peak at 1364 cm^{-1} is strongly decreased. Only small shifts in the peak positions occur upon heating to 425 K. Under these conditions, four peaks can be clearly identified at 1340, 1420, 1456, and 1583 cm^{-1}. Further heating to 600 K causes a decrease in the intensities of all three peaks but no significant shifts of the peak positions. This is also the case after annealing to 720 K.

In order to get additional structural information, we also studied the polarization dependence of the IR spectra of the chemisorbed species produced by annealing the sample to 425 K after dosing 2–3 layers of CH_3COOH or CD_3COOD onto the surface. The results and experimental geometry are provided in Fig. 9. As one can see clearly from Fig. 9(a), the peak near 1465 cm^{-1} shows a strong polarization dependence and can only be produced by using IR light with an electric field, E, parallel to the surface normal. No significant polarization dependence was observed for the other peaks. In comparing these spectra to those using perdeutero-acetic acid, the peak at 1340 cm^{-1} disappeared completely and the peak at 1420 decreased in intensity as shown in Fig. 9(b). Therefore, we assign these two peaks to C–H deformations. The C–H stretching vibration cannot be observed in our experiment, presumably due to the low intensity of this mode. It is well known that the presence of the COO group decreases the IR cross section for the C–H stretching vibration but increases the IR cross section for C–H deformations. The peaks at 1583 and 1465 cm^{-1} for CH_3COOH shift to 1572 and 1447 cm^{-1} for CD_3COOD. Consistent with the results for CH_3COOH, the peak at 1447 cm^{-1} in Fig. 9(b) shows a clear polarization dependence. These two peaks are correlated to the two C–O stretching vibrations of the COO group.

IV. DISCUSSION

A. Adsorbed species

Acetic acid can exist in several different forms. In the liquid, it mainly forms cyclic dimers.[41] However, indications for open chain dimers have also been found.[42] In the solid state, it forms a chainlike polymer.[35,36] The C=O stretching vibration provides some sensitivity to the chemical environment and it has often been correlated to the different forms of acetic acid.[35–44] For the monomer and dimer in the gas phase, this mode is found at 1788 and 1730 cm^{-1}, respec-

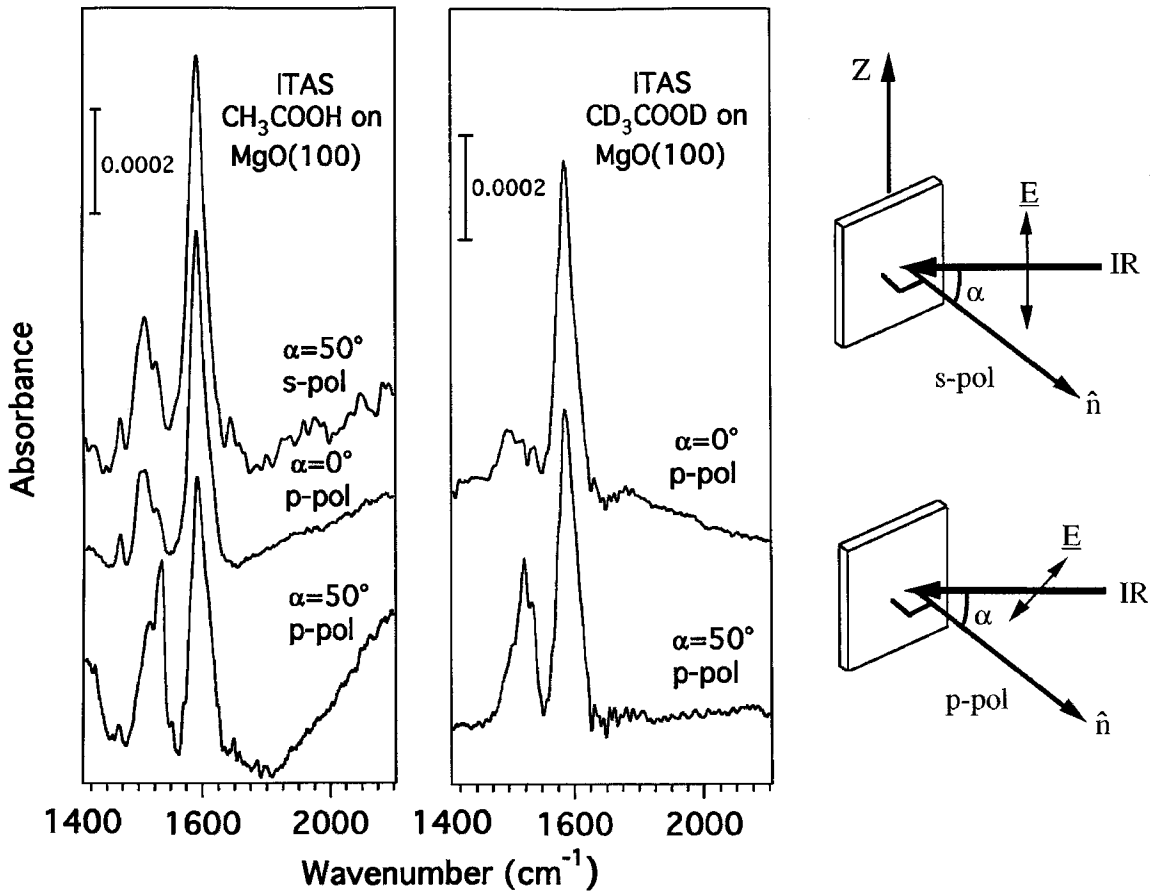

FIG. 9. Polarization dependence in FT-ITAS of the carboxyl stretching modes of the chemisorbed acetate species produced by heating a multilayer of acetic acid on MgO(100).

tively. This vibration for the dimer in the liquid phase shifts to 1715 cm^{-1}. The chain form in solid acetic acid shows a C═O stretching vibration at 1648 cm^{-1}. For the multilayer state of acetic acid on MgO(100), we found this mode at 1701 cm^{-1}. Therefore, the acetic acid is probably present as a dimer in the condensed multilayer on MgO(100). However, some acetic acid might be present in the chain form as a polymer in the adlayer as indicated by the peak at 1653 cm^{-1}. Another possible explanation for this peak is that the frequency of the C═O stretching vibration of the dimer is modified by the MgO surface. On the Pt(111) surface, the C═O stretch vibration of the dimer was assigned to a peak at 1675 cm^{-1}.[39] In any case, species associated with the peak at 1653 cm^{-1} show a higher desorption temperature than the multilayer species. In addition to these two possible states, a peak at 1746 cm^{-1} was always observed. The high frequency of this peak indicates a monomeric form of the adsorbate. Moreover, the intense peak at 1279 cm^{-1} is clearly correlated with either the peak at 1653 or 1746 cm^{-1}. Since this peak is due to the O–H in-plane deformation and the spectra were taken with the *E* field parallel to surface, the high intensity of this peak indicates that the molecular plane of the acetic acid corresponding to this state is parallel to the surface. Unfortunately, the frequency of this peak is independent of whether or not there is a hydrogen bond.[43] Therefore, no further information can be gained from this peak regarding the form of this adsorbed state.

In addition to the weakly bound, molecularly adsorbed species, a strongly bound chemisorbed species is also observed which is stable on the surface to 600 K. The very low frequency of the C═O stretching vibration indicates the formation of acetate, CH_3COO, on the surface. The peaks correlated to acetate decrease in intensity upon annealing to high temperature but without significant shifts of the peak positions or the formation of new peaks. This particular aspect of our results is in excellent agreement with previous studies that were carried out above 300 K.[15,31–33]

B. Adsorption geometry of the chemisorbed state, the acetate species

Adsorbed acetate can be bound to the surface either by using only one oxygen (monodentate form) or both oxygen atoms (bidentate form) as illustrated in Fig. 10. The carboxylate complex has been studied extensively,[45] and a strong correlation has been found between the splitting of the carboxylate-stretching frequencies and the bonding configuration. For the bidentate linkage isomer, the splitting is found to be between 130–180 cm^{-1}. The monodentate isomer shows a splitting larger than 200 cm^{-1}. For instance, the splitting of the two stretching vibrations for acetate in the complex $[Co(NH_3)_5CH_3CO_2](ClO_4)_2$ is 223 cm^{-1}.[45] In Table II, we provide the vibrational frequencies of acetate adsorbed on single crystal and powdered MgO.[26,30] For comparison,

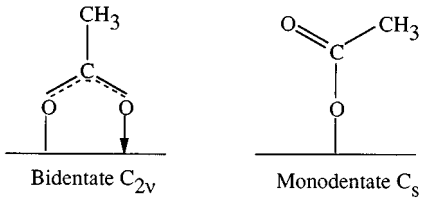

FIG. 10. Possible bidentate and monodentate linkage isomers of acetate on the MgO surface.

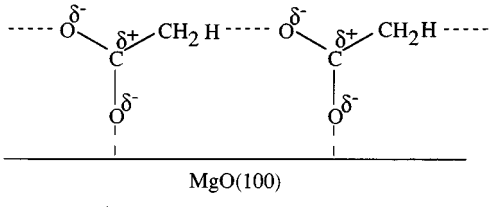

FIG. 11. Proposed structure and intermolecular interactions between adsorbed acetate species on MgO(100).

the frequencies for free acetate ion in CH_3COONa are also given.[46,47] The small splitting between the symmetric and asymmetric COO stretching vibrations observed in our experiment implies that acetate is bound in the bidentate configuration. However, this assignment is not consistent with the polarization dependence of the spectra for this species. For a bidentate geometry, one expects that both symmetric and asymmetric COO stretching vibrations would show a strong polarization dependence. In changing from an *E* vector parallel to the surface to an *E* vector perpendicular to the surface, the symmetric stretching vibration should gain in intensity, while the asymmetric stretching vibration should lose intensity. Although the symmetric stretching vibration behaves in this manner in our experiment, we didn't see any significant polarization dependence for the asymmetric stretching vibration. Therefore, the polarization experiments exclude the possibility of a bidentate geometry.

If acetate is bound as a monodentate species on the surface as illustrated in Fig. 10, it is not meaningful to refer to the two stretching vibrations as symmetric and asymmetric vibrations. Rather, we have two well separated vibrations due to the C–O and C═O bonds. Especially in our case where the acetate is strongly bound to the surface, resonance is limited. Therefore, the polarization direction of the C–O stretching vibration is along the C–O axis and the polarization direction for the C═O stretching vibration is along the C═O bond direction. In the monodentate adsorption geometry illustrated in Fig. 10, one expects a strong polarization dependence for the C–O stretching vibration but a very weak polarization dependence for the C═O stretching vibration because its direction is very close to the so-called ''magic angle'' where no polarization dependence can be observed. Our experimental results are in perfect agreement with the polarization dependence expected for a monodentate bonding geometry. Therefore, we conclude that acetate is bound to MgO(100) in a monodentate configuration. The monodentate geometry has been previously observed for formate adsorbed on ZnO(0001),[25] MgO(100),[26] and NiO(100).[17] It is interesting to note that carboxylate species prefer to be bound to oxide surfaces in a monodentate configuration, while on metallic substrates the bidentate isomer has often been found. This preference of monodentate over bidentate forms on oxide surfaces has been rationalized using geometric and electronic arguments.[2] The distance between the two oxygen atoms in free carboxylate is much smaller than the distance between the surface cation sites on oxides and bidentate bonding would cause substantial strain in the ring.[25]

TABLE II. Stretching vibrational frequencies of the carboxyl group in acetate.

System	ν_s (cm^{-1})[a]	ν_{as} (cm^{-1})	$\Delta\nu$ (cm^{-1})	Ref.
CH_3COO(a) on MgO(100)	1456(1447)	1583(1572)	127(125)	This work
CH_3COO(a) on MgO(100)	1449	1579	130	26
CH_3COO(a) on MgO	1445	1565	120	30
CH_3COONa	1413(1406)	1556(1545)	143(139)	46
$(CH_3COO)_2Cu$	1420	1591	171	47

[a]Values given in parentheses are for the deuterated species.

A question remains concerning the small splitting of the two stretching vibrations in the carboxyl (COO) group of the adsorbed acetate radical on MgO(100). It is surprising that this splitting is even smaller than in the free acetate ion. However, even though a large splitting of the carboxylate-stretching frequencies is usually characteristic of monodentate coordination, a similar small splitting was observed previously for acetate in a monodentate configuration in $Ni(H_2O)_4(CH_3CO_2)_2$. In this complex, the two stretching vibrations occur at 1520 and 1413 cm^{-1} with a splitting of only 107 cm^{-1}.[48] This small separation was attributed to the strong intramolecular hydrogen bonding between the uncoordinated acetate oxygen atom and a water molecule.[48] Such hydrogen bonding might also be present in our system. A schematic drawing of one possible hydrogen bonding configuration is shown in Fig. 11. As one can see, we propose hydrogen bonding between the uncoordinated acetate oxygen atom and a hydrogen atom from the methyl group. The adsorbed acetate can form either a dimer or long chains utilizing this hydrogen bonding interaction.

Since MgO is a typical ionic crystal, the main contribution to the cohesive energy is from electrostatic forces (Madelung energy). Even on the surface, the charge separation has been found to be very high (80–90% of the nominal ionic value of ± 2 a.u.).[49] Therefore, the adsorbed molecule is bound to the surface mainly by electrostatic forces.[50–52] To be strongly bound to the surface, as in the case of acetate on MgO, a large charge separation such as that illustrated in Fig. 11 is necessary. This charge separation is certainly induced by the presence of the ionic surface and is also stabilized by the Madelung energy. This large charge separation will also facilitate the hydrogen bonding indicated. To summarize, we conclude that the ionic surface of MgO(100) induces a strong charge separation in adsorbed acetate and stabilizes hydrogen bonding between neighboring adsorbed acetate species. The presence of hydrogen bonding and large charge separa-

tion in the adsorbate cause a small splitting (energy difference) of the carboxylate stretching vibrations.

C. Reaction of adsorbed acetate

Our TPD results show that ketene is the major reaction product of acetate decomposition at high temperature, consistent with the earlier results of Peng and Barteau.[32] However, in addition to ketene desorption, we found significant molecular desorption of acetic acid and also water desorption near 300 K. The water is presumably formed from lattice oxygen and hydrogen produced by the heterolytic dissociation of acetic acid. IR results show that adsorbed acetate is stable on the surface up to 500 K. Heating to higher temperatures causes a decrease in the IR peaks associated with acetate, however, no new features were observed. These results indicate that the observed ketene desorption in TPD is controlled by reaction (acetate decomposition, ketene formation) rate-limited kinetics, rather than desorption rate-limited kinetics.

Peng and Barteau[32] proposed that ketene is formed via a unimolecular process:

$$CH_3COOH(g) \xrightarrow{300\ K} CH_3COO(a)+H(a), \tag{1}$$

$$CH_3COO(a)+H(a) \xrightarrow{520\ K} CH_2CO(g)+H_2O(g). \tag{2}$$

However, this mechanism is not consistent with our finding that a substantial amount of water desorbs well below 300 K. In addition, the hydroxyl group, OH(a), on MgO(100) produced by water adsorption recombines and desorbs between 170 and 400 K.[15,16] Therefore, at 520 K the only remaining adsorbed species on the surface is acetate, $CH_3COO(a)$.

We propose an alternative reaction path for ketene formation:

$$CH_3COOH(g) \xrightarrow{130\ K} CH_3COO(ad)+H(ad), \tag{3}$$

$$2\ H(ad)+O(lattice) \xrightarrow{300\ K} H_2O(g), \tag{4}$$

$$2\ CH_3COO(ad) \xrightarrow{520\ K} 2\ CH_2CO(g)+H_2O(g)+O(lattice), \tag{5a}$$

or

$$2\ CH_3COO(ad) \xrightarrow{520\ K} CH_2CO(g)+CH_3COOH(g) + O(lattice). \tag{5b}$$

Our proposed reaction path is supported by the IR results that indicate a large charge separation and hydrogen bonding within the adlayer as discussed in Sec. IV. Due to hydrogen bonding, one acetate can abstract a hydrogen atom from the methyl group of an adjacent acetate forming acetic acid and a $CH_2COO(a)$ intermediate. The acetic acid can either desorb molecularly from the surface or dissociate to ketene and water at high surface temperatures. The $CH_2COO(a)$ intermediate dissociates by cleaving the C–O bond to leave oxygen on the surface (restoring vacancies produced by water desorption) and desorb ketene. The net reaction of acetic acid on MgO(100) is a stoichiometric reaction and does not require the net consumption of lattice oxygen.

V. CONCLUSION

The adsorption and reaction of acetic acid on MgO(100) has been studied using FTIR and TPD. Acetic acid dissociates heterolytically upon adsorption at any temperature above 130 K. The chemisorbed acetate species produced from dissociative adsorption of acetic acid is stable on the surface up to 500 K. FTIR is a powerful probe of the adsorbate vibrations and we observed four well-resolved peaks between 1000 and 2000 cm^{-1}, correlated to C–H deformation and carboxylate stretching vibrations, in contrast to the barely discernible features seen in previous HREELS investigations of this system. In addition, we measured the polarization dependence of the vibrational modes for adsorbed acetate and determined that acetate is bound as a monodentate ligand. We also used the small splitting of the carboxylate stretching vibration to determine that a reasonably large charge separation is present and intermolecular hydrogen bonding occurs within the adlayer. Upon heating, adsorbed acetate dehydrates cleanly to ketene via a bimolecular reaction pathway.

ACKNOWLEDGMENT

This work was supported by the U.S. Army Research Office.

[1] H. H. Kung, *Transition Metal Oxides: Surface Chemistry and Catalysis*, *Studies in Surface Science and Catalysis* (Elsevier, Amsterdam, 1990), Vol. 45.
[2] V. E. Henrich and P. A. Cox, *The Surface Science of Metal Oxides* (Cambridge University Press, Cambridge, 1993).
[3] *Adsorption on Ordered Surfaces of Ionic Solids and Thin Films*, Vol. 33 of Springer Series in Surface Science, edited by H.-J. Freund and E. Umbach (Springer, Heidelberg, 1993).
[4] E. I. Solomon, P. M. Jones, and J. A. May, Chem. Rev. **93**, 2623 (1993).
[5] H. Kuhlenbeck, G. Odörfer, R. M. Jaeger, G. Illing, M. Menges, Th. Mull, H.-J. Freund, M. Pölchen, V. Staemmler, S. Witzel, C. Scharfschwerdt, K. Wennemann, T. Liedtke, and M. Neumann, Phys. Rev. B **43**, 1969 (1991).
[6] C. Xu, M. Hassel, M. Kuhlenbeck, and H.-J. Freund, Surf. Sci. **258**, 23 (1991).
[7] C. Xu, B. Dillmann, H. Kuhlenbeck, and H.-J. Freund, Phys. Rev. Lett. **67**, 3551 (1991).
[8] H. Kuhlenbeck, C. Xu, B. Adam, M. Hassel, B. Dillmann, H.-J. Freund, U. A. Ditzinger, H. Neddermeyer, M. Neuber, and M. Neumann, Ber. Bunsenges. Phys. Chem. **96**, 15 (1992).
[9] M. Bäumer, D. Cappus, G. Illing, H. Kuhlenbeck, and H.-J. Freund, J. Vac. Sci. Technol. A **10**, 2407 (1992).
[10] D. Cappus, C. Xu, D. Ehrlich, B. Dillmann, C. A. Ventrice Jr., K. Al-Shamery, H. Kuhlenbeck, and H.-J. Freund, Chem. Phys. **177**, 533 (1993).
[11] F. Winkelmann, S. Wohlrab, J. Libuda, M. Bäumer, D. Cappus, M. Menges, K. Al-Shamery, H. Kuhlenbeck, and H.-J. Freund, Surf. Sci. **307/309**, 1148 (1994).
[12] D. W. Goodman, Surf. Sci. **299/300**, 837 (1994).
[13] M.-C. Wu, J. S. Corneille, C. A. Estrada, J.-W. He, and D. W. Goodman, Chem. Phys. Lett. **182**, 472 (1991).
[14] M.-C. Wu, C. A. Estrada, and D. W. Goodman, Phys. Rev. Lett. **67**, 2910 (1991).
[15] M.-C. Wu and D. W. Goodman, Catal. Lett. **15**, 1 (1992).
[16] M.-C. Wu, C. A. Estrada, J. S. Corneille, and D. W. Goodman, J. Chem. Phys. **96**, 3892 (1992).

[17] C. M. Truong, M.-C. Wu, and D. W. Goodman, J. Chem. Phys. **97**, 9447 (1993).
[18] X. Xu and D. W. Goodman, Surf. Sci. **282**, 323 (1993).
[19] X. Xu, S. M. Vesecky, and D. W. Goodman, Science **258**, 788 (1992).
[20] K. Coulter and D. W. Goodman, Catal. Lett. **16**, 191 (1992).
[21] P. A. Thiry, M. Liehr, J. J. Pireaux, and R. Caudano, Phys. Rev. B **29**, 4824 (1984).
[22] M. Liehr, P. A. Thiry, J. J. Pireaux, and R. Caudano, J. Vac. Sci. Technol. A **2**, 1079 (1986).
[23] M. Liehr, P. A. Thiry, J. J. Pireaux, and R. Caudano, Phys. Rev. B **33**, 5682 (1986).
[24] P. A. Cox, W. R. Flavell, A. A. Williams, and R. G. Egdell, Surf. Sci. **152/153**, 784 (1985).
[25] W. T. Petrie and J. M. Vohs, Surf. Sci. **245**, 315 (1991).
[26] W. T. Petrie and J. M. Vohs, Surf. Sci. **259**, L750 (1991).
[27] A. A. Davydov, *Infrared Spectroscopy of Adsorbed Species on the Surface of Transition Metal Oxides* (Wiley, New York, 1990).
[28] D. N. Mirlin, in *Surface Polaritons: Electromagnetic Waves at Surfaces and Interfaces*, edited by V. M. Agranovich and D. L. Mills (North-Holland, New York, 1982).
[29] S. L. Parrott, J. W. Rogers, Jr., and J. M. White, Appl. Surf. Sci. **1**, 443 (1978).
[30] D. G. Walmsley, W. J. Nelson, N. M. D. Brown, S. de Cheveigné, S. Gauthier, J. Klein, and A. Léger, Spectrochim. Acta **37A**, 1015 (1981).
[31] X. D. Peng and M. A. Barteau, Surf. Sci. **224**, 327 (1989).
[32] X. D. Peng and M. A. Barteau, Catal. Lett. **7**, 395 (1990).
[33] X. D. Peng and M. A. Barteau, Langmuir **7**, 1426 (1991).
[34] C. Xu, J. Wang, P. M. Blass, H. Ferkel, C. Wittig, H. Reisler, and B. E. Koel (unpublished).
[35] M. Haurie and A. Novak, Spectrochim. Acta **21**, 1217 (1965).
[36] P. F. Krause, J. E. Katon, J. M. Rogers, and D. B. Phillips, Appl. Spectrosc. **31**, 110 (1977).
[37] S. Bratoz, D. Hadzi, and N. Sheppard, Bull. Sci. Acad. PRF. Yougoslavie **1**, 71 (1953).
[38] S. Bratoz, D. Hadzi, and N. Sheppard, Spectrochim. Acta **8**, 249 (1956).
[39] Q.-Y. Gao and J. C. Hemminger, Surf. Sci. **248**, 45 (1991).
[40] J. G. Chen, J. E. Crowell, and J. T. Yates, Jr., Surf. Sci. **172**, 733 (1986).
[41] H. Bertagnolli, Chem. Phys. Lett. **93**, 287 (1982).
[42] L. J. Bellamy, R. F. Lake, and R. J. Pace, Spectrochim. Acta **19**, 443 (1963).
[43] R. C. Herman and R. Hofstadter, J. Chem. Phys. **7**, 460 (1939).
[44] M. Ovaska, J. Phys. Chem. **88**, 5981 (1984).
[45] M. Linhard and B. Rau, Z. Anorg. Chem. **271**, 121 (1953).
[46] K. Ito and H. J. Bernstein, Can. J. Chem. **34**, 170 (1956).
[47] G. Costa, E. Pauluzzi, and A. Puxeddu, Gazz. Chim. Ital. **87**, 885 (1957).
[48] J. Catterick and P. Thornton, Adv. Inorg. Chem. Radiochem. **20**, 291 (1977).
[49] U. Birkenheuer, J. C. Boettger, and N. Rösch, J. Chem. Phys. **100**, 6826 (1994).
[50] M. I. McCarthy and A. C. Hess, J. Chem. Phys. **96**, 6010 (1992).
[51] G. Pacchioni, G. Cogliandro, and P. S. Bagus, Int. J. Quantum Chem. **42**, 1115 (1992).
[52] N. Rösch, K. M. Neyman, and U. Birkenheuer, in *Adsorption on Ordered Surfaces of Ionic Solids and Thin Films*, Ref. 3.